

---



---

## Kinematic Analysis of Solar-Neighborhood Stars Based on RAVE4 Data

V.V. Bobylev and A.T. Bajkova

*Pulkovo Astronomical Observatory, St. Petersburg, Russia*

**Abstract**—We consider stars with radial velocities, proper motions, and distance estimates from the RAVE4 catalogue. Based on a sample of more than 145000 stars at distances  $r < 0.5$  kpc, we have found the following kinematic parameters:  $(U, V, W)_{\odot} = (9.12, 20.80, 7.66) \pm (0.10, 0.10, 0.08)$  km s<sup>−1</sup>,  $\Omega_0 = 28.71 \pm 0.63$  km s<sup>−1</sup> kpc<sup>−1</sup>, and  $\Omega'_0 = -4.28 \pm 0.11$  km s<sup>−1</sup> kpc<sup>−2</sup>. This gives the linear rotation velocity  $V_0 = 230 \pm 12$  km s<sup>−1</sup> (for the adopted  $R_0 = 8.0 \pm 0.4$  kpc) and the Oort constants  $A = 17.12 \pm 0.45$  km s<sup>−1</sup> kpc<sup>−1</sup> and  $B = -11.60 \pm 0.77$  km s<sup>−1</sup> kpc<sup>−1</sup>. The 2D velocity distributions in the  $UV$ ,  $UW$ , and  $VW$  planes have been constructed using a local sample,  $r < 0.25$  kpc, consisting of  $\sim 47000$  stars. A difference of the  $UV$  velocity distribution from the previously known ones constructed from a smaller amount of data has been revealed. It lies in the fact that our distribution has an extremely enhanced branch near the Wolf 630 peak. A previously unknown peak at  $(U, V) = (-96, -10)$  km s<sup>−1</sup> and a separate new feature in the Wolf 630 stream, with the coordinates of its center being  $(U, V) = (30, -40)$  km s<sup>−1</sup>, have been detected.

## INTRODUCTION

The distribution of stellar space velocities in the solar neighborhood has a complex structure. First, characteristic peaks associated with known open clusters are identified (Skuljan et al. 1999; Famaey et al. 2005; Bobylev and Bajkova 2007; Antoja et al. 2008; Bobylev et al. 2010). Second, a bimodal velocity distribution is observed. Some authors believe this bimodality to have a dynamical nature related to the influence of the central Galactic bar on the motion of stars close to the Suns (Dehnen 1999, 2000; Fux 2001; Chakrabarty 2007; Gardner and Flinn 2010).

Highly accurate space velocities of stars, implying the availability of their proper motions, radial velocities, and distances, are required to study these phenomena. Other characteristics of stars, such as the metallicity indices and age estimates, are also important. Data from several catalogues have contributed greatly to the solution of the problem. These include the proper motions and parallaxes from the Hipparcos catalogue (ESA 1997; van Leeuwen 2007), the radial velocities from the PCRV compilation (Gontcharov 2006), and the age estimates and metallicity indices from the Geneva–Copenhagen survey (Holmberg et al. 2007, 2009). These data were used to analyze the space velocities of  $\sim 20000$  solar-neighborhood stars (Bobylev and Bajkova 2007; Antoja et al. 2008; Klement et al. 2008; Francis and Anderson 2009; Bobylev et al. 2010). The next big step is

expected to be made after the implementation (approximately after 2018) of the GAIA space project, when the parallaxes, radial velocities, and proper motions will be measured for millions of stars with a microarcsecond accuracy.

The RAVE (RAAdial Velocity Experiment) project plays a significant role in studying stellar streams. It is a large-scale ground-based project aimed at determining the radial velocities of faint stars with an accuracy of  $\sim 1\text{--}2 \text{ km s}^{-1}$ . Observations in the southern hemisphere started in 2003. Four releases of this catalogue (DR1–DR4) have been published Since then.

Analysis of the RAVE DR1 data (Steinmetz et al. 2006) revealed a previously unknown stream in the region of “fast” stars ( $V \approx -160 \text{ km s}^{-1}$ ) with an age of  $\sim 13 \text{ Gyr}$  (Klement et al. 2008). It was designated as KFR08 (Klement et al. 2008). Having analyzed the RAVE DR2 (Zwitter et al. 2008) and RAVE DR3 (Siebert et al. 2011) data, for which the distances were estimated by Burnett et al. (2011), Antoja et al. (2012) detected a previously unknown stream at  $(U, V) = (92, -22) \text{ km s}^{-1}$ .

The errors in the spectrophotometric distances of stars from the RAVE catalogue are about 30% or more. Nevertheless, various authors have shown that a number of important kinematic parameters can be estimated quite reliably based on RAVE data (Coşkunoğlu et al. 2011; Pasetto et al. 2012; Binney et al. 2014b).

The goal of this paper is to test the space velocities of stars from the latest version, RAVE DR4 (Kordopatis et al. 2013). This catalogue contains the original radial velocities, proper motions, and photometric distances for 425561 stars. We want to examine how well the Galactic rotation parameters can be determined from distant stars and to analyze the 2D velocity distributions in the  $UV$ ,  $UW$ , and  $VW$  planes for nearby stars.

## METHODS

From observations we know three projections of the stellar velocity: the radial velocity  $V_r$  as well as the two velocity components  $V_l = 4.74r\mu_l \cos b$  and  $V_b = 4.74r\mu_b$  directed along the Galactic longitude  $l$  and latitude  $b$  and expressed in  $\text{km s}^{-1}$ . Here, the coefficient 4.74 is the ratio of the number of kilometers in an astronomical unit to the number of seconds in a tropical year, and  $r$  is the star’s heliocentric distance in kpc. The proper motion components  $\mu_l \cos b$  and  $\mu_b$  are expressed in milliarcseconds per year ( $\text{mas yr}^{-1}$ ). The velocities  $U$ ,  $V$ , and  $W$  directed along the rectangular Galactic coordinate axes are calculated via the components  $V_r$ ,  $V_l$ , and  $V_b$ :

$$\begin{aligned} U &= V_r \cos l \cos b - V_l \sin l - V_b \cos l \sin b, \\ V &= V_r \sin l \cos b + V_l \cos l - V_b \sin l \sin b, \\ W &= V_r \sin b + V_b \cos b, \end{aligned} \tag{1}$$

where  $U$  is directed from the Sun to the Galactic center,  $V$  is in the direction of Galactic rotation, and  $W$  is directed toward the north Galactic pole.

To determine the parameters of the Galactic rotation curve, we use the equations derived from Bottlinger’s formulas, in which the angular velocity  $\Omega$  is expanded in a series to terms of the second order of smallness in  $r/R_0$ :

$$\begin{aligned} V_r &= -U_\odot \cos b \cos l - V_\odot \cos b \sin l \\ &\quad - W_\odot \sin b + R_0(R - R_0) \sin l \cos b \Omega_0'' + 0.5R_0(R - R_0)^2 \sin l \cos b \Omega_0''', \end{aligned} \tag{2}$$

$$V_l = U_\odot \sin l - V_\odot \cos l - r\Omega_0 \cos b \\ + (R - R_0)(R_0 \cos l - r \cos b)\Omega'_0 + 0.5(R - R_0)^2(R_0 \cos l - r \cos b)\Omega''_0, \quad (3)$$

$$V_b = U_\odot \cos l \sin b + V_\odot \sin l \sin b \\ - W_\odot \cos b - R_0(R - R_0) \sin l \sin b \Omega'_0 - 0.5R_0(R - R_0)^2 \sin l \sin b \Omega''_0, \quad (4)$$

Here,  $R$  is the distance from the star to the Galactic rotation axis:

$$R^2 = r^2 \cos^2 b - 2R_0 r \cos b \cos l + R_0^2. \quad (5)$$

In this paper, we take the Galactocentric distance of the Sun to be  $R_0 = 8.0 \pm 0.4$  kpc, as estimated by Foster and Cooper (2010).

To identify statistically significant signals from the main clumps in the  $UV$  velocity distributions, we use a wavelet transform, which is known as a powerful tool for filtering spatially localized signals (Chui 1997; Vityazev 2001).

The wavelet transform of a 2D distribution  $f(U, V)$  consists in its decomposition into analyzing wavelets  $\psi(U/a, V/a)$ , where  $a$  is the coefficient that allows a wavelet of a certain scale to be separated from the entire family of wavelets characterized by the same shape  $\psi$ . The wavelet transform  $w(\xi, \eta)$  is defined as a correlation function in such a way that at any given point  $(\xi, \eta)$  in the  $UV$  plain, we have one real value of the following integral:

$$w(\xi, \eta) = \int_{-\infty}^{\infty} \int_{-\infty}^{\infty} f(U, V) \psi\left(\frac{U - \xi}{a}, \frac{V - \eta}{a}\right) dU dV, \quad (6)$$

called the wavelet coefficient at point  $(\xi, \eta)$ . Obviously, in the case of finite discrete maps that we are dealing with, their number is finite and equal to the number of square bins on the map.

As an analyzing wavelet we use the traditional wavelet called the Mexican Hat (MHAT). The 2D MHAT wavelet is described by the expression

$$\psi(d/a) = \left(2 - \frac{d^2}{a^2}\right) e^{-d^2/2a^2}, \quad (7)$$

where  $d^2 = U^2 + V^2$ . The wavelet (7) is obtained by differentiating the Gaussian function twice. The main property of the wavelet  $\psi$  is that its integral over  $U$  and  $V$  is zero, which allows any clumps in the distribution being studied to be detected. If the distribution being analyzed is uniform, then all coefficients of the wavelet transform will be zero.

## DATA

Following Williams et al. (2013), we take the stars satisfying the following criteria to select candidates without significant random observational errors:

$$|V_r| < 600 \text{ km s}^{-1}, \\ |\mu_\alpha, \mu_\delta| < 400 \text{ mas yr}^{-1}, \\ |e_{\mu_\alpha}, e_{\mu_\delta}| < 20 \text{ mas yr}^{-1}. \quad (8)$$

In the RAVE DR4 catalogue containing the proper motions from various sources, we used those copied from the UCAC4 catalogue (Zacharias et al. 2013).

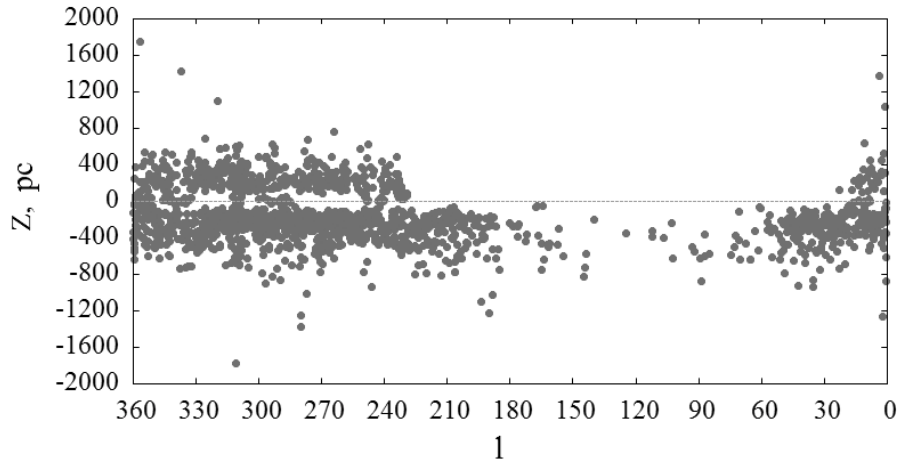


Figure 1: Distribution of a small sample of stars from the RAVE DR4 catalogue perpendicular to the Galactic plane

As the RAVE program was being performed, several versions of spectrophotometric distance estimates were published (Breddels et al. 2010; Zwitter et al. 2010; Burnett and Binney 2010; Burnett et al. 2011; Binney et al. 2014a). From the catalogue we take the distances expressed in kpc (there are also the parallaxes and distance moduli) and determined by Binney et al. (2014a). According to the estimates by these authors, the distance errors are 15–20% for hot dwarfs, they reach 20–30% for the coolest dwarfs, and these errors are even larger for giants.

The technique for estimating the individual ages of stars from the RAVE DR4 catalogue is described in Burnett and Binney (2010) and Binney et al. (2014a). This technique consists in comparing the positions of stars on the Hertzsprung-Russell diagram with suitable theoretical isochrones. The technique was applied both to main-sequence stars and to giants. The Bayesian approach is used for this purpose; it consists in simultaneously seeking for six unknowns: the metal abundance, the stellar age, the stellar mass, the heliocentric distance of the star, and the Galactic coordinates of the star. Such a problem is solved by the maximum likelihood method. The solution requires (a) observational data and (b) a priori information, i.e., a model. The Padova isochrones are ultimately used to determine the ages. As was noted by Burnett and Binney (2010) and Binney et al. (2014a), the distances and ages for giants are estimated with the largest errors compared to those for dwarfs. Kordopatis et al. (2013) point out that the age and distance estimates obtained for stars from the RAVE4 catalogue are of interest only from a statistical point of view.

A peculiarity of the RAVE catalogue is a highly nonuniform spatial distribution of stars, because only the southern hemisphere of the celestial sphere is observed. The distribution of a small ( $8.5 < \lg t < 8.75$ ) sample of stars from the RAVE DR4 catalogue perpendicular to the Galactic plane is shown in Fig. 1. As can be seen from the figure, a significant space in the range of longitudes  $30^\circ - 240^\circ$  remains unfilled in the northern Galactic hemisphere.

Table 1: Galactic rotation parameters found from five samples from the distance range  $r$ : 0.5–3 kpc

Parameters	$J - K < 0.5$	$J - K \geq 0.5$	$\lg t < 9.4$	$\lg t: 9.4\text{--}9.8$	$9.8 < \lg t$
	$ Z  < 0.3 \text{ kpc}$		$ Z  < 0.6 \text{ kpc}$		
$U_{\odot}, \text{ km s}^{-1}$	$11.82 \pm 0.48$	$13.48 \pm 0.42$	$11.58 \pm 0.37$	$13.01 \pm 0.20$	$12.16 \pm 0.43$
$V_{\odot}, \text{ km s}^{-1}$	$18.47 \pm 0.36$	$22.02 \pm 0.24$	$15.60 \pm 0.28$	$22.94 \pm 0.16$	$31.35 \pm 0.36$
$W_{\odot}, \text{ km s}^{-1}$	$8.34 \pm 0.29$	$6.09 \pm 0.19$	$7.19 \pm 0.23$	$6.87 \pm 0.12$	$7.76 \pm 0.36$
$\Omega_0, \text{ km s}^{-1} \text{ kpc}^{-1}$	$23.52 \pm 0.69$	$20.40 \pm 0.37$	$23.25 \pm 0.44$	$22.07 \pm 0.20$	$22.99 \pm 0.39$
$\Omega'_0, \text{ km s}^{-1} \text{ kpc}^{-2}$	$-3.14 \pm 0.12$	$-3.15 \pm 0.06$	$-3.05 \pm 0.08$	$-3.05 \pm 0.04$	$-2.48 \pm 0.08$
$\Omega''_0, \text{ km s}^{-1} \text{ kpc}^{-3}$	$0.79 \pm 0.29$	$1.06 \pm 0.12$	$0.33 \pm 0.16$	$0.51 \pm 0.07$	$0.33 \pm 0.11$
$\sigma_0, \text{ km s}^{-1}$	36.0	36.8	33.6	38.4	48.0
$N_{\star}$	15933	38896	21202	96107	24842
$V_0, \text{ km s}^{-1}$	$188 \pm 11$	$163 \pm 9$	$186 \pm 10$	$177 \pm 9$	$184 \pm 9$
$A, \text{ km s}^{-1} \text{ kpc}^{-1}$	$12.56 \pm 0.48$	$12.60 \pm 0.25$	$12.18 \pm 0.34$	$12.19 \pm 0.16$	$-9.91 \pm 0.31$
$B, \text{ km s}^{-1} \text{ kpc}^{-1}$	$-10.96 \pm 0.84$	$-7.79 \pm 0.45$	$-11.06 \pm 0.55$	$-9.88 \pm 0.07$	$-13.08 \pm 0.49$

As is well known (Antoja et al. 2012; Williams et al. 2013), the spatial distribution of stars from the RAVE catalogue resembles a cone with its axis along the Galactic  $Z$  axis. For example, only a few stars very close to the Sun are located below approximately 150 pc. This effect is also seen in Fig. 1 as a poorly filled band extended along the equator. Thus, the constraints on  $Z$  play an important role in selecting the necessary stars from the RAVE catalogue.

## RESULTS

### Galactic Rotation

To determine the Galactic rotation parameters, we produced several samples within 3 kpc of the Sun for solving the system of equations (2)–(4). The upper boundary of the interval  $r = 3 \text{ kpc}$  was chosen here in such a way that the errors of the stellar proper motions (they increase with distance when converted to  $\text{km s}^{-1}$ ) did not dominate in the sample. The results are reflected in Tables 1 and 2.

Table 1 presents the results obtained from stars with heliocentric distances  $r$  from 0.5 to 3 kpc. Here, we did not use any stars at  $r < 0.5 \text{ kpc}$  to reduce the influence of old low-mass dwarfs, which are represented in the catalogue mostly at close distances (Fig. 12 in Binney et al., 2014a). Columns 2 and 3 of the table present the results obtained from two samples that were selected under the condition  $|Z| < 0.3 \text{ kpc}$  and that differ in  $(J - K)$  color index. Note that the  $(J - K)$  color index is a temperature index, while  $(J - K) = 0.5$  corresponding to a temperature  $T_{eff} \approx 5000 \text{ K}$ . Columns 4–6 of the table present the results obtained from three samples that were selected under the condition  $|Z| < 0.6 \text{ kpc}$  and that differ in age.

As can be seen from the table, there are only  $\sim 55000$  stars in the zone  $r = 0.5 - 3 \text{ kpc}$ ,

Table 2: Galactic rotation parameters found from samples of stars with various ages taken from the distance range  $r < 3$  kpc and  $|Z| < 0.6$  kpc

Parameters	lg $t$ : 8.5–9.0	lg $t$ : 9.0–9.4	lg $t$ : 9.4–9.8	9.8 < lg $t$
$U_{\odot}$ , km s $^{-1}$	$10.84 \pm 0.36$	$10.66 \pm 0.22$	$10.46 \pm 0.11$	$9.77 \pm 0.18$
$V_{\odot}$ , km s $^{-1}$	$13.05 \pm 0.33$	$14.71 \pm 0.19$	$21.48 \pm 0.09$	$25.73 \pm 0.17$
$W_{\odot}$ , km s $^{-1}$	$6.90 \pm 0.28$	$7.17 \pm 0.16$	$7.19 \pm 0.08$	$8.14 \pm 0.16$
$\Omega_0$ , km s $^{-1}$ kpc $^{-1}$	$25.21 \pm 0.59$	$23.98 \pm 0.34$	$24.36 \pm 0.13$	$24.53 \pm 0.34$
$\Omega'_0$ , km s $^{-1}$ kpc $^{-2}$	$-3.76 \pm 0.12$	$-3.17 \pm 0.07$	$-3.33 \pm 0.03$	$-2.66 \pm 0.08$
$\Omega''_0$ , km s $^{-1}$ kpc $^{-3}$	$0.00 \pm 0.25$	$-0.08 \pm 0.14$	$0.11 \pm 0.05$	$-0.65 \pm 0.11$
$\sigma_0$ , km s $^{-1}$	26.8	30.7	35.2	40.1
$N_{\star}$	8975	35385	183631	59741
$V_0$ , km s $^{-1}$	$202 \pm 12$	$192 \pm 10$	$195 \pm 10$	$196 \pm 10$
$A$ , km s $^{-1}$ kpc $^{-1}$	$15.05 \pm 0.49$	$12.66 \pm 0.29$	$13.31 \pm 0.12$	$10.65 \pm 0.30$
$B$ , km s $^{-1}$ kpc $^{-1}$	$-10.17 \pm 0.77$	$-11.32 \pm 0.44$	$-11.05 \pm 0.18$	$-13.87 \pm 0.45$

$|Z| < 0.3$  kpc. The parameters found from these two samples have virtually no differences between themselves. There are already more stars in the zone  $r = 0.5 - 3$  kpc,  $|Z| < 0.6$  kpc; therefore, we used three samples of different ages.

We can see that the components of the Sun’s peculiar velocity  $U_{\odot}, V_{\odot}, W_{\odot}$  are determined well from all samples.  $U_{\odot}$  and  $W_{\odot}$  remain almost constant.  $V_{\odot}$  increases with age of the sample stars, reflecting the well-known asymmetric drift effect. The second derivative of the angular velocity of Galactic rotation  $\Omega''_0$  is determined well.

The lower rows of Table 1 give the linear velocity of the solar neighborhood around the Galactic center  $V_0 = R_0\Omega_0$ , along with the Oort constants  $A = 0.5R_0\Omega'_0$  and  $B = \Omega_0 + 0.5R_0\Omega'_0$ . The table gives the error per unit weight  $\sigma_0$ . This quantity characterizes the dispersion of the residuals when the system of equations (2)–(4) is solved by the least-squares method. Its value is usually close to the dispersion of the residual velocities for the sample stars averaged over all directions (the “cosmic” velocity dispersion) and correlates well with the age of the sample stars.

Table 2 gives the Galactic rotation parameters found by solving the system of equations (2)–(4) for four samples of stars with various ages at  $r < 3$  kpc under the condition  $|Z| < 0.6$  kpc. It can be seen from the number of stars (287732) that the bulk of the RAVE DR4 catalogue is covered.

When working on the sample of youngest stars, we noticed that the error per unit weight  $\sigma_0$  increased significantly at an age  $\lg t < 8.5$ , reaching more than 35 km s $^{-1}$ . Therefore, we do not use the age interval  $\lg t < 8.5$ ; however, there are very few such stars.

In general, we see that including nearby ( $r < 0.5$  kpc) stars led to an increase in  $\Omega_0$  (and, accordingly, in  $V_0$ ), but the second derivative of the angular velocity of Galactic rotation  $\Omega''_0$  ceased to be determined. Since Eqs. (2)–(4) contain the distance squared at this unknown,  $\Omega''_0$  can be determined only at large sample radii,  $r > 2$  kpc. Therefore, using stars at  $r < 0.5$  kpc, of course, gives nothing for the determination of  $\Omega''_0$ . However, in the solution for the age interval  $\lg t = 9.4 - 9.8$ , all of the parameters being determined

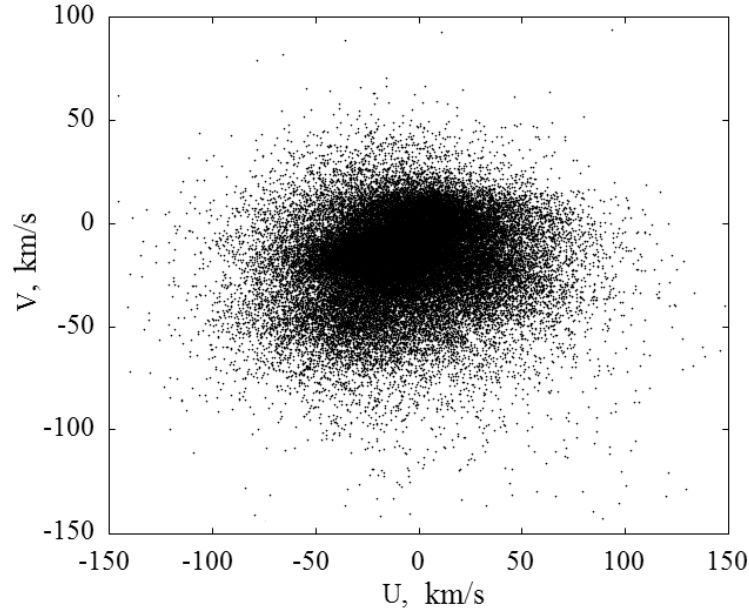


Figure 2:  $UV$  velocity distribution for a sample of 47304 stars within 250 pc of the Sun. The velocities are given relative to the Sun.

have the smallest errors (compared to other age intervals), and even the sign of  $\Omega_0''$  is positive.

To analyze the 2D velocity distributions, we must correct the velocities  $U$  and  $V$  for the Galactic differential rotation. However, since we take stars close to the Sun, no farther than 500 pc, for this purpose, it will suffice to use only two parameters, for example,  $\Omega_0$  and  $\Omega_0'$  or the two Oort constants  $A$  and  $B$ , to take into account the Galactic rotation.

To this end, we took 145807 stars at  $r < 0.5$  kpc and found a solution of the system of equations (2)–(4) with five unknowns (without  $\Omega_0''$ ):

$$\begin{aligned} (U_\odot, V_\odot, W_\odot) &= (9.12, 20.80, 7.66) \pm (0.10, 0.10, 0.08) \text{ km s}^{-1}, \\ \Omega_0 &= 28.71 \pm 0.63 \text{ km s}^{-1} \text{ kpc}^{-1}, \\ \Omega_0' &= -4.28 \pm 0.11 \text{ km s}^{-1} \text{ kpc}^{-2}, \end{aligned} \tag{9}$$

This gives the linear rotation velocity of the Sun around the Galactic center  $V_0 = 230 \pm 12$  km s<sup>-1</sup> for the adopted  $R_0 = 8.0 \pm 0.4$  kpc as well as  $A = 17.12 \pm 0.45$  km s<sup>-1</sup> kpc<sup>-1</sup> and  $B = -11.60 \pm 0.77$  km s<sup>-1</sup> kpc<sup>-1</sup>. Based on this solution, below we correct the sample of local stars for the Galactic rotation.

## Velocity Distributions

To analyze the 2D velocity distributions, we took stars close to the Sun. These stars are located within 250 pc of the Sun.  $U, V, W$  are the residual velocities, i.e., they were corrected for the Galactic rotation with the parameters from solution (9). In addition, the random errors for each of the velocities  $U, V, W$  do not exceed 30 km s<sup>-1</sup>. The  $UV$

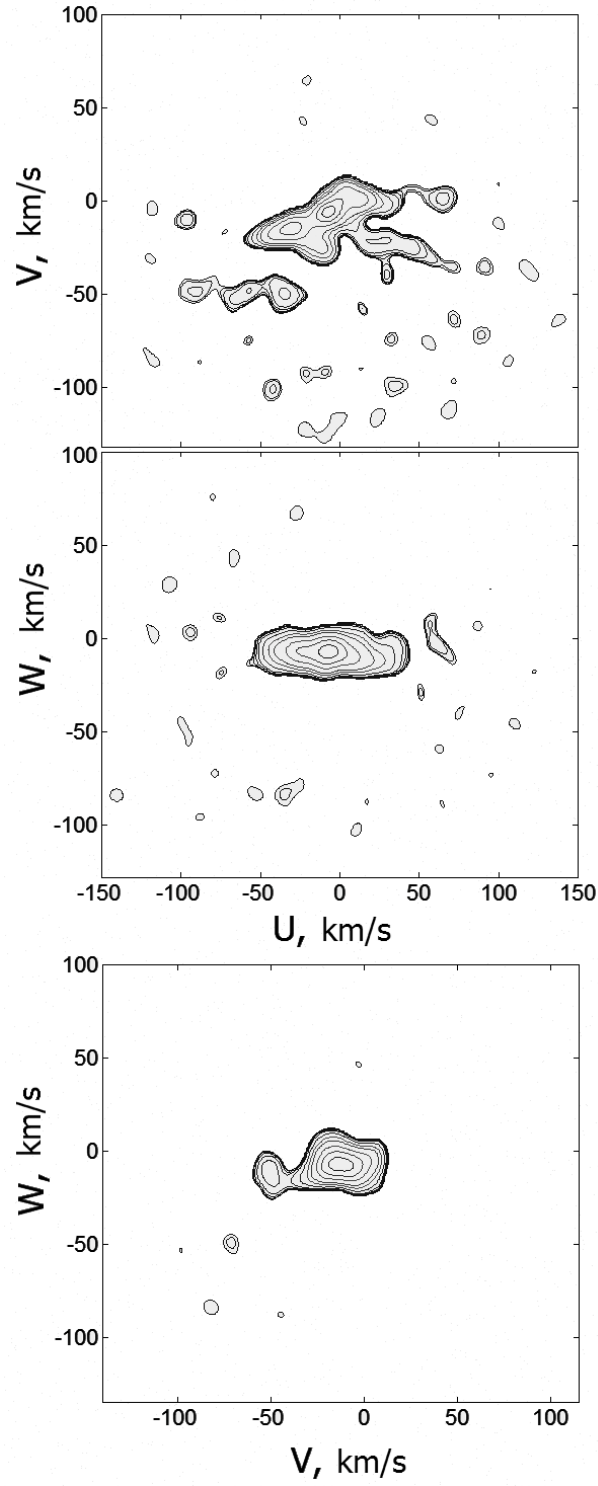


Figure 3: Smoothed wavelet maps of  $UV$ ,  $UW$ , and  $VW$  velocities for a sample of 47304 stars within 250 pc of the Sun. The velocities are given relative to the Sun.



velocity distribution for the stars of this sample containing 47304 stars is shown in Fig. 2.

Figure 3 presents the wavelet maps of  $UV$ ,  $UW$ , and  $VW$  velocities for our sample of 47304 stars. The following system of levels on the graphs was chosen: 0.0025, 0.005, 0.01, 0.02, 0.04, 0.1, 0.2, 0.3, 0.4, 0.5, 0.7, and 0.9.

Table 3 gives the coordinates of the main peaks in the  $UV$  velocity plane and an approximate number of stars ( $N_*$ ) in each of the peaks. The identification with the peaks from Antoja et al. (2012) is reflected in the last column of the table. Note that the random errors of the peak centers are approximately equal in our paper and in Antoja et al. (2012). As follows from Table 2 in Antoja et al. (2012), these errors increase dramatically as one recedes from the distribution center. For example, the errors in each of the coordinates are 0.1–0.2 km s<sup>-1</sup> at the point with coordinates  $(U, V) = (0, 0)$  km s<sup>-1</sup>, while toward the map boundaries, at velocities  $U \approx 120$  km s<sup>-1</sup> or  $V \approx 120$  km s<sup>-1</sup>, the errors reach  $\sim 10$  km s<sup>-1</sup>. Therefore, the classical peaks at the map center, which have their own names, for example, Pleiades, Hyades, or Sirius, are easily identified. Closer to the map edges, the discrepancy in peak coordinates becomes increasingly significant, making the identification difficult.

For example, the coordinates of stream no. 12 are  $(U, V) = (92, -22) \pm (3.5, 1.4)$  km s<sup>-1</sup> (Antoja et al. 2012). We identified it with the feature at  $(U, V) = (91, -35) \pm (4.2, 1.5)$  km s<sup>-1</sup> on our map, where this isolated feature is clearly seen and has two contours. Thus, there is no doubt whatsoever that the identification is correct.

The coordinates of stream no. 15 are  $(U, V) = (60, -72) \pm (3.3, 4.7)$  km s<sup>-1</sup> (Antoja et al. 2012). We identify it with the feature at  $(U, V) = (72, -64) \pm (3.2, 3.0)$  km s<sup>-1</sup> on our map. Given the errors, the coincidence is seen to be close.

One would think that there should be no difference between the maps from Antoja et al. (2012) and our maps—in both cases, the data were taken from the RAVE catalogue after all. However, different systems of distances were used in these two cases, leading to differences in the observed velocities  $U, V, W$ .

Note that all of the isolated peaks with at least two contours on the  $UV$  velocity map (Fig. 3) are reflected in one form or another in Table 3. If, however, the peak on the  $UV$  velocity map (Fig. 3) has only one contour (quite a low significance), then we did not include it in the table. The weak peak no. 24 that we identified with peak no. 13 from Antoja et al. (2012) constitutes an exception. As follows from Fig. 3 and Table 3, a chain of four peaks is clearly seen in the region of the Hercules stream: nos. 5, 8, 10, and 24. The situation is similar in the region of the Wolf 630 stream traced by five peaks: nos. 6, 7, 12, 14, and 17.

## DISCUSSION

First of all, it should be noted that the components of the Sun’s group velocity we found,  $(U, V, W)_\odot$ , agree well with the results of other authors.

Having analyzed the RAVE DR3 stars that belong to the Galactic thin disk with a high probability, Coşkunoğlu et al. (2011) found  $(U, V, W)_\odot = (8.50, 13.38, 6.49) \pm (0.29, 0.43, 0.26)$  km s<sup>-1</sup>. They should be compared with the results in the second ( $\lg t =$

Table 3: Coordinates of the main peaks in the  $UV$  velocity plane

No	$U$	$V$	$N_{\star}$	Name
	km s <sup>-1</sup>			
1	-7	-6	1800	Coma Berenices
2	-30	-15	1500	Hyades
3	10	1	1290	Sirius
4	-13	-24	1480	Pleiades
5	-35	-50	390	Hercules II
6	29	-21	624	Wolf 630
7	43	-24	290	Dehnen98 (No14)
8	-57	-48	248	Hercules I
9	65	1	272	$\gamma$ Leo
10	-90	-49	108	$\varepsilon$ Ind
11	-42	-101	115	$\eta$ Cep
12	20	-22	450	Dehnen98 (No6)
13	14	-58	75	HR 1614
14	30	-40	395	
15	-96	-10	190	
16	91	-35	40	Antoja12 (No12)
17	71	-35	400	
18	72	-64	25	Antoja12 (No15)
19	35	-99	99	
20	32	-74	85	
21	-10	-82	83	
22	-61	-72	39	
23	84	-74	49	
24	-120	-32	42	Antoja12 (No13)

8.5 – 9.0) or third ( $\lg t = 9.0 - 9.4$ ) columns of Table 2. There is also good agreement with the results of a detailed analysis of the velocities  $(U, V, W)_{\odot}$  based on RAVE data (Pasetto et al. 2012; Karaali et al. 2014). Of interest is Fig. 7 from Karaali et al. (2014), where the velocity  $V_{\odot}$  is plotted against the  $Z$  coordinate, with the minimum value of this velocity being  $\sim 10$  km s<sup>-1</sup> at  $Z = 0$  kpc. Pasetto et al. (2012) concluded that two velocities,  $U_{\odot}$  and  $W_{\odot}$ , remained virtually unchanged at various constraints imposed on the sample stars. These authors found  $(U, W)_{\odot} = (10.9, 7.2) \pm (1.0, 1.3)$  km s<sup>-1</sup>. The velocity  $V_{\odot}$  is known to reflect the lag of the centroids behind the Sun (asymmetric drift); therefore, this velocity increases with increasing age of the sample stars. According to present-day estimates (Schönrich et al. 2010; Bobylev and Bajkova 2014), the minimum value of this velocity is  $V_{\odot} \approx 12$  km s<sup>-1</sup>.

At present, there is a sample of about 100 masers whose trigonometric parallaxes were measured by VLBI with a very high accuracy, with a mean error of  $\pm 20$  microarcseconds and, some of them, with a record errors of  $\pm 5$  microarcseconds. Having analyzed these masers, Reid et al. (2014) found the solar velocity to be  $V_0 = 240 \pm 8$  km s<sup>-1</sup> ( $R_0 = 8.34 \pm 0.16$  kpc). Based on a smaller number of masers, Honma et al. (2012) obtained

an estimate of  $V_0 = 238 \pm 14 \text{ km s}^{-1}$  ( $R_0 = 8.05 \pm 0.45 \text{ kpc}$ ). This is the velocity  $V_0$  for the youngest fraction of the Galactic disk, because the masers used are associated with young massive protostars. The parameters of solution (9) agree with these estimates.

The clumps in the  $UV$  velocity plane have been repeatedly analyzed by various authors using the parallaxes and proper motions from the Hipparcos catalogue (ESA 1997) and, occasionally, with the inclusion of stellar radial velocities. Note, for example, the papers by Dehnen (1998), Skuljan et al. (1999), Famaey et al. (2005), Antoja et al. (2008), Zhao et al. (2009), Bobylev et al. (2010), etc.

When preparing Table 3, we compared the coordinates of the peaks with those from Dehnen (1998), Zhao et al. (2009), and Antoja et al. (2012). The presence of the peak detected by Antoja et al. (2012) is confirmed. Moreover, we detected a previously unknown at  $(U, V) = (-96, -10) \pm (5.1, 1.5) \text{ km s}^{-1}$  and a separate feature in the Wolf 630 stream at  $(U, V) = (30, -40) \pm (3.0, 3.0) \text{ km s}^{-1}$ .

In general, we can conclude that there is an important difference of our  $UV$  velocity distribution from the previously known ones constructed from a smaller amount of data from the Hipparcos catalogue. This difference lies in the presence of an extremely developed branch in the region of the Wolf 630 peak. It can be seen from Fig. 3 that the boundary of this region extends up to  $U \approx 70 \text{ km s}^{-1}$ . When other data are analyzed, this boundary usually did not extend farther than  $U \approx 50 \text{ km s}^{-1}$  (Dehnen 1998; Bobylev et al. 2010; Bubar and King 2010; Antoja et al. 2012).

It follows from Fig. 3 that the  $UW$  velocity ellipsoid is parallel to the Galactic plane, The  $VW$  velocity distribution is bimodal, because the Hercules stream is very powerful and, hence, forms a separate clump here. No such effect was observed on the corresponding map constructed from Hipparcos data (Dehnen 1998; Bobylev et al. 2010).

## CONCLUSIONS

We considered stars from the RAVE4 catalogue with known radial velocities, proper motions, and distance estimates. We showed that the solar peculiar velocity components  $U_\odot, V_\odot, W_\odot$ , the angular velocity of Galactic rotation at the solar distance  $\Omega_0$ , and its first derivative  $\Omega'_0$  are satisfactorily determined from stars within 3 kpc of the Sun. The second derivative  $\Omega''_0$  is determined well only from samples of distant stars at distances of 0.5–3 kpc;  $\Omega_0$  decreases in this case. The difficulties (the impossibility to simultaneously determine all the parameters of interest to us) are related to the complex space distribution of objects from the RAVE catalogue.

We obtained one of the solutions based on a sample of 183 631 stars with ages in the interval  $9.4 < \lg t < 9.8$ :  $(U, V, W)_\odot = (10.46, 21.48, 7.19) \pm (0.11, 0.09, 0.08) \text{ km s}^{-1}$ ;  $\Omega_0 = 24.36 \pm 0.13 \text{ km s}^{-1} \text{ kpc}^{-1}$ ;  $\Omega'_0 = -3.33 \pm 0.03 \text{ km s}^{-1} \text{ kpc}^{-2}$ ;  $\Omega''_0 = 0.11 \pm 0.05 \text{ km s}^{-1} \text{ kpc}^{-3}$ . This gives the linear rotation velocity of the Sun's around the Galactic center  $V_0 = 195 \pm 10 \text{ km s}^{-1}$  for the adopted  $R_0 = 8.0 \pm 0.4 \text{ kpc}$ .

When using nearer stars having, on average, smaller errors in their space velocities, the rotation velocity of the solar neighborhood around the Galactic center turns out to be higher. We found the following kinematic parameters from a sample of 145 807 stars at distances  $r < 0.5 \text{ kpc}$ :  $(U, V, W)_\odot = (9.12, 20.80, 7.66) \pm (0.10, 0.10, 0.08) \text{ km s}^{-1}$ ,

$\Omega_0 = 28.71 \pm 0.63 \text{ km s}^{-1} \text{ kpc}^{-1}$ , and  $\Omega'_0 = -4.28 \pm 0.11 \text{ km s}^{-1} \text{ kpc}^{-2}$ . This gives  $V_0 = 230 \pm 12 \text{ km s}^{-1}$  (for  $R_0 = 8.0 \pm 0.4 \text{ kpc}$ ),  $A = 17.12 \pm 0.45 \text{ km s}^{-1} \text{ kpc}^{-1}$ , and  $B = -11.60 \pm 0.77 \text{ km s}^{-1} \text{ kpc}^{-1}$ .

It was noticed that the error per unit weight  $\sigma_0$  increased considerably at an age  $\lg t < 8.5$ , reaching approximately  $35 \text{ km s}^{-1}$ . This is larger than the expected error for stars of such an age, about  $25 \text{ km s}^{-1}$ . This means that either the distance estimates or the ages are not reliable for the youngest stars from the RAVE catalogue.

We constructed the 2D velocity distributions in the  $UV$ ,  $UW$ , and  $VW$  planes. The  $UV$  velocity distribution differs from the previously known distributions constructed from a smaller amount of data from the Hipparcos catalogue. This difference lies in the fact that our distribution shows an extremely enhanced branch in the Wolf 630 region. We detected a previously unknown stream at  $(U, V) = (-96, -10) \text{ km s}^{-1}$  and a separate new feature in the Wolf 630 stream with coordinates  $(U, V) = (30, -40) \text{ km s}^{-1}$ .

## ACKNOWLEDGMENTS

We are grateful to the referees for their useful remarks that contributed to an improvement of our paper.

## REFERENCES

1. T. Antoja, F. Figueras, D. Fernández, and J. Torra, *Astron. Astrophys.* 490, 135 (2008).
2. T. Antoja, A. Helmi, O. Bienaymé, J. Bland-Hawthorn, B. Famaey, K. Freeman, B.K. Gibson, G. Gilmore, E.K. Grebel, et al., *Mon. Not. R. Astron. Soc.* 426, L1 (2012).
3. J. Binney, B. Burnett, G. Kordopatis, P.J. McMillan, S. Sharma, T. Zwitter, O. Bienaymé, J. Bland-Hawthorn, et al., *Mon. Not. R. Astron. Soc.* 437, 351 (2014a).
4. J. Binney, B. Burnett, G. Kordopatis, M. Steinmetz, G. Gilmore, O. Bienaymé, J. Bland-Hawthorn, B. Famaey, et al., *Mon. Not. R. Astron. Soc.* 439, 1231 (2014b).
5. V.V. Bobylev and A.T. Bajkova, *Astron. Rep.* 51, 372 (2007).
6. V.V. Bobylev, A.T. Bajkova, and A.A. Mylläri, *Astron. Lett.* 36, 27 (2010).
7. V.V. Bobylev and A.T. Bajkova, *Mon. Not. R. Astron. Soc.* 441, 142 (2014).
8. M.A. Breddels, M.C. Smith, A. Helmi, O. Bienaymé, J. Binney, J. Bland-Hawthorn, C. Boeche, B.C.M. Burnett, et al., *Astron. Astrophys.* 511, A90 (2010).
9. E.J. Bubar and J.R. King, *Astron. J.* 140, 293 (2010).
10. B. Burnett and J. Binney, *Mon. Not. R. Astron. Soc.* 407, 339 (2010).
11. B. Burnett, J. Binney, S. Sharma, M. Williams, T. Zwitter, O. Bienaymé, J. Bland-Hawthorn, K.C. Freeman, et al., *Astron. Astrophys.* 532, A113 (2011).
12. D. Chakrabarty, *Astron. Astrophys.* 467, 145 (2007).
13. C.K. Chui, *Wavelets: A Mathematical Tool for Signal Analysis* (SIAM, Philadelphia, PA, 1997).
14. B. Coğkunoğlu, S. Ak, S. Bilir, S. Karaali, E. Yaz, G. Gilmore, G.M. Seabroke, O. Bienaymé, et al., *Mon. Not. R. Astron. Soc.* 412, A1237 (2011).
15. W. Dehnen, *Astron. J.* 115, 2384 (1998).
16. W. Dehnen, *Astrophys. J.* 524, L35 (1999).
17. W. Dehnen, *Astron. J.* 119, 800 (2000).
18. B. Famaey, A. Jorissen, X. Luri, M. Mayor, S. Udry, H. Dejonghe, and C. Turon, *Astron. Astrophys.* 430, 165 (2005).

19. T. Foster, and B. Cooper, The Dynamic Interstellar Medium: A Celebration of the Canadian Galactic Plane Survey, eds R. Kothes, T.L. Landecker, A.G. Willis, ASP Conf. Ser. 438, 16 (2010).
20. C. Francis and E. Anderson, *New Astron.* 14, 615 (2009).
21. R. Fux, *Astron. Astrophys.* 373, 511 (2001).
22. E. Gardner and C. Flinn, *Mon. Not. R. Astron. Soc.* 405, 545 (2010).
23. G.A. Gontcharov, *Astron. Lett.* 32, 759 (2006).
24. The HIPPARCOS and Tycho Catalogues, ESA SP-1200 (1997).
25. J. Holmberg, B. Nordström, and J. Andersen, *Astron. Astrophys.* 475, 519 (2007).
26. J. Holmberg, B. Nordström, and J. Andersen, *Astron. Astrophys.* 501, 941 (2009).
27. M. Honma, T. Nagayama, K. Ando, T. Bushimata, Y.K. Choi, T. Handa, T. Hirota, H. Imai, T. Jike, et al., *Publ. Astron. Soc. Jpn.* 64, 136 (2012).
28. S. Karaali, S. Bilir, S. Ak, E. Yaz Gökçe, Ö. Önal, and T. Ak, *Publ. Astron. Soc. Austral.* 31, 13 (2014).
29. R. Klement, B. Fuchs, and H.-W. Rix, *Astrophys. J.* 685, 261 (2008).
30. G. Kordopatis, G. Gilmore, M. Steinmetz, C. Boeche, G.M. Seabroke, A. Siebert, T. Zwitter, J. Binney, P. de Laverny, et al., *Astron. J.* 146, A134 (2013).
31. F. van Leeuwen, *Astron. Astrophys.* 474, 653 (2007).
32. S. Pasetto, E.K. Grebel, T. Zwitter, C. Chiosi, G. Bertelli, O. Bienaymé, G. Seabroke, J. Bland-Hawthorn, et al., *Astron. Astrophys.* 547, A71 (2012).
33. M.J. Reid, K.M. Menten, A. Brunthaler, X.W. Zheng, T.M. Dame, Y. Xu, Y. Wu, B. Zhang, et al., *Astrophys. J.* 783, 130 (2014).
34. R. Schönrich, J. Binney, and W. Dehnen, *Mon. Not. R. Astron. Soc.* 403, 1829 (2010).
35. A. Siebert, M.E.K. Williams, A. Siviero, W. Reid, C. Boeche, M. Steinmetz, J. Fulbright, U. Munari, T. Zwitter, et al., *Astron. J.* 141, 187 (2011).
36. J. Skuljan, J.B. Hearnshaw, and P.L. Cottrell, *Mon. Not. R. Astron. Soc.* 308, 731 (1999).
37. M. Steinmetz, T. Zwitter, A. Seibert, F.G. Watson, K.C. Freeman, U. Munari, R. Campbell, M. Williams, et al., *Astron. J.* 132, 1645 (2006).
38. V.V. Vityazev, *Wavelet-Analysis of Time Series* (SPb. Gos. Univ., St.-Petersburg, 2001) [in Russian].
39. M.E.K. Williams, M. Steinmetz, J. Binney, A. Siebert, H. Enke, B. Famaey, I. Minchev, R.S. de Jong, et al., *Mon. Not. R. Astron. Soc.* 436, 101 (2013).
40. N. Zacharias, C. Finch, T. Girard, A. Henden, J.L. Bartlett, D.G. Monet, and M.I. Zacharias, *Astron. J.* 145, 44 (2013).
41. J. Zhao, G. Zhao, and Y. Chen, *Astrophys. J.* 692, L113 (2009).
42. T. Zwitter, A. Siebert, U. Munari, K.C. Freeman, A. Siviero, F.G. Watson, J.P. Fulbright, R.F.G. Wyse, et al., *Astron. J.* 136, 421 (2008).
43. T. Zwitter, G. Matijević, M.A. Breddels, M.C. Smith, A. Helmi, U. Munari, O. Bienaymé, J. Binney, J. Bland-Hawthorn, et al., *Astron. Astrophys.* 522, A54 (2010).